

03/06/2003  
ORIAS, 2807 1110A CT - 05

EE-3	1297
------	------



MILITARY TECHNICAL COLLEGE  
CAIRO - EGYPT

DIGITAL COMPUTER TRANSIENT MODEL OF THREE-PHASE  
GTO THYRISTOR INVERTER FEEDING AN INDUCTION MOTOR

S.A. GAWISH \*and M.A. MORSY SHANAB\*\*

ABSTRACT

Although the autosequentially commutated current source inverter (ASCI) is widely used with the induction motor for speed control, it is limited for high power and high frequency induction motor drives, mainly due to the commutation capacitors in the inverter circuit. For its advantages over the conventional inverters, the Gate Turn off (GTO) thyristor inverters has attracted attention in recent years. The computer model of the current source GTO thyristor inverter feeding an induction motor is simulated. The developed digital computer program has three subprograms, each of them has a special function but linking them together provides the output variables. The main subprogram contains the input data and the logic concerned with the operation of the six GTO thyristors, six diodes, three-phase bridge. The second subprogram deals with the specification of the differential equations according to the conducting states of the GTO's and diodes of the inverter circuit determined in the main subprogram. In the third subprogram, the set of differential equations is solved according to the fourth order Runge-kutta method. The output results will be a main factor for the determination of the conducting state of each thyristor in the main subprogram. This operation will be repeated every time step. The computed results compared favorably with those obtained recently in practice.

\*D.Sc. ,Dept. of EL. Power. Military Technical College, Cairo-Egypt.  
\*\*Ph.D. Head, Dept. of EL-Power Military Technical College, Cairo-Egypt.

## 1. CIRCUIT CONFIGURATION

In the last five years, the GTO thyristor has attracted attention because of its higher frequency response, improved efficiency and smaller size compared with the ASCI [1]. It has been used for the variable speed operation of fans, pumps and transit car drives aimed at a fast-response speed control of induction motors with energy savings [2].

Since the GTO is turned-off by a signal through its gate, it is similar to the forced commutated inverter from a modeling point of view. By further modification of the forced commutated inverter program a digital simulation of the GTO thyristor inverter feeding an induction motor was obtained for the first time.

For comparison reasons, the same system tested in practice is used for simulation under steady state conditions. This system shown in Fig.1 contains the energy rebound circuit which is usually employed with ASCI in order to clamp the voltage spikes produced in commutation and is used not only to rebound the load reactive power to the dc link in pulses, but also to return the power in the load to the ac source [3].

The system parameters are:

For the induction motor : Power -3.7 Kw, Current -15 A, Voltage-200 V  
Frequency- 50 Hz, p.f. -0.84, Pole-4

$$R_A = R_B = R_C = 5\Omega$$

$$\text{Time step} = 10^{-4} \text{ sec.}$$

$$L_A = L_B = L_C = 15 \text{ mH}$$

$$V_A = V_m \sin(\omega t + \psi)$$

$$V_B = V_m \sin(\omega t - 2\pi/3 + \psi)$$

$$V_C = V_m \sin(\omega t + 2\pi/3 + \psi)$$

where :

$$V_m = 35 \text{ V}$$

$$\omega = 2\pi f, f = 50 \text{ Hz}$$

$$V_S = \text{the output dc voltage of the three-phase rectifier bridge} = 90 \text{ V}$$

$$L_{dc} = \text{inductance of the dc link} = 100 \text{ mH}$$

$$R_{dc} = \text{resistance of the dc link inductor} = 0.2 \Omega$$

## 2. DESCRIPTION OF THE PROGRAM

This developed digital computer program has three subprograms, each of them has a special function but linking them together provides the output variables  $i_A, i_B, i_C, i_{dc}, V_A, V_B, V_C$  and  $V_{dc}$ .

## 2.1. The Main Subprogram

This is the main part of the program which contains the input data ( $R_A, R_B, R_C, L_A, L_B, L_C, V_S, R_{dc}, L_{dc}$ , frequency, time step, accuracy, turn off current limit, firing angles, initial values for line currents and its time derivatives). The main subprogram contains the logic concerned with the operation of the six GTO thyristors, six diodes, three-phase bridge.

Each individual GTO thyristor satisfies the operating conditions of positive polarity voltage between its anode and cathode and a firing signal will conduct, otherwise, it will be blocking. Once a GTO thyristor is fired, it will not stop conducting unless the current falls below the turn off limit, which is accomplished by another gate signal. The whole logic of an individual GTO thyristor operation is shown in Fig.2. The program prints out the conducting thyristors and diodes (Table 1). Since this is a kind of forced commutated inverter, when a thyristor is turned off, the other GTO thyristor on the same phase will fail to conduct and current will continue to flow in the opposite direction for a short time in the return-diode. When the current reaches zero, the other thyristor will then conduct provided that the triggering signal is still present. At that moment the current will change its direction in that phase. This delay of conduction is due to the inductance of the load [4].

## 2.2. The Second Subprogram

The second subprogram deals with the specification of the differential equation according to:

- How many GTO thyristors and diodes are conducting
- For each conducting condition, the differential equation is determined every time step, according to  $L_{eq}/R_{eq}$  of the current loop.

Throughout the subprogram  $L_{eq}/R_{eq}$  is named  $\tau_1, \tau_2, \dots$  according to the equivalent circuit. If  $L_{eq}/R_{eq} < 10^{-3}$  sec., i.e., less than ten times the time step, the circuit is considered resistive. If  $L_{eq}/R_{eq} > 10^{-3}$  sec., then the time constant will be taken into consideration. If the load is purely resistive, three GTO thyristors will be conducting in the sequence 561, 612, 123, ... etc. That means each GTO thyristor will be conducting for  $180^\circ$  then it will be forced to the blocking condition [5]. If the load is inductive, there will be a delay of thyristor conduction during which the current will be carried by the parallel diode and the state of three conducting thyristor is not valid, but from the differential equations point of view the sequence 561, 612, 123, ..... etc. is still valid.

It is obvious that there are many differential equation sets, each set represents one conducting state. One set of differential equations will be illustrated and the other sets will be derived in a similar way.

## 3. Circuit Equations

The GTO thyristors will be fired in the sequence  $G_1, G_2, G_3, \dots$  at  $60^\circ$  apart. There are many cases of conducting state of the circuit. As an example,  $G_1, G_2$ , and  $D_3$ , will be conducting. The circuit diagram for this case is shown in Fig. 3.

$$i_A + i_B + i_C = 0 \quad (1)$$

$$\frac{di_A}{dt} + \frac{di_B}{dt} + \frac{di_C}{dt} = 0 \quad (2)$$

$$i_C = i_{dc}$$

$$\frac{di_C}{dt} = \frac{di_{dc}}{dt} \quad (3)$$

$$R_{dc} i_{dc} + L_{dc} \frac{di_{dc}}{dt} - R_A i_A - L_A \frac{di_A}{dt} + V_A - V_C + L_C \frac{di_C}{dt} + R_C \frac{di_C}{dt} = V_S \quad (4)$$

and

$$-R_A i_A - L_A \frac{di_A}{dt} + V_A - V_B + L_B \frac{di_B}{dt} + R_B i_B = 0 \quad (5)$$

Solving (2), (3), (4) and (5) for  $\frac{di_A}{dt}$ ,  $\frac{di_B}{dt}$ ,

$\frac{di_C}{dt}$  and  $\frac{di_{dc}}{dt}$  yields:

$$\frac{di_A}{dt} = \frac{1}{L + L_{dc}(L_A + L_B)} \{ L_B [ V_A - V_C - V_S - R_A i_A + i_C (R_C + R_{dc}) ] + (L_C + L_{dc}) [ V_A - V_B - i_A (R_A + R_B) - i_C R_B ] \} \quad (6)$$

Similarly,

$$\frac{di_B}{dt} = \frac{1}{L + L_{dc}(L_B + L_A)} \{ L_A [ V_B - V_C - R_B i_B + i_C (R_C + R_{dc}) ] + (L_C + L_{dc}) [ V_B - V_A - i_B (R_B + R_A) - i_C R_A ] \} \quad (7)$$

where:

$$L = L_A L_B + L_B L_C + L_C L_A$$

and

$$\frac{di_C}{dt} = - \left( \frac{di_A}{dt} + \frac{di_B}{dt} \right) \quad (8)$$

$$\frac{di_{dc}}{dt} = \frac{di_C}{dt} \quad (9)$$

Then the fourth order Runge-Kutta method is used to solve for  $i_A, i_B, i_C, i_{dc}$ , from  $\frac{di_A}{dt}$ ,  $\frac{di_B}{dt}$ ,  $\frac{di_C}{dt}$ , and  $\frac{di_{dc}}{dt}$ .

The resulting currents along with its time derivatives will be used to determine the circuit's next conducting state.

#### 4. Comparison Between the Obtained Results and the Recently Obtained Practical Ones

The practical results obtained recently by Matsuse, Hashimoto and Kubota [3] are shown in Fig. 4. while Fig. 6. shows the simulation results overlaid on the experimental results. Comparing  $i_u, V_{uv}, e_d$  and  $i_{DBR}$  of Fig. 4 with the corresponding  $i_A, V_{AB}, V_{dc}$  and  $i_{dc}$  shown in Figs. 5. (a), (b), (c) and (d), respectively, one can conclude that the computed results compared favorably with those obtained recently in practice. The little differences in the dc current and the dc voltage are mainly due to the choice of the smoothing inductor and also because the input voltage to the inverter was taken as a constant (90 volts) while in practice it was the actual output

of a three-phase rectifier. Figures 5 (a-d) show the simulation results of the CSI-GTO inverter motor system.

### 5. CONCLUSIONS

For its advantages over the conventional inverters, the GTO thyristor inverter has attracted attention in recent years. The simulation of the current source GTO thyristor inverter, presented here, feeding an induction motor can easily be used for the study of such a system since it produces simulation results as the real system. The computed results compared favorably with those obtained recently in practice.

### 6. REFERENCES

1. Shashani, M.M., " Harmonic Reduction Using Gate Turn-off Thyristors in Static VAR Compensators", PH.D., University of Missouri, Columbia, 1982.
2. Honbu, M., Matuda, Y. and Miyazaky, K., " Parallel Operation Techniques of GTO Inverter Sets for Large AC Motor Drives", IEEE Trans., Ind. Appl., Vol. IA-19, No.2, March/ April, 1983.
3. Matsuse, K., Hashimoto, H. and Kubota, H., "Current Source GTO Inverter With Energy Rebound", IEE Inter, Conf. on Power Electronics and Variable-Speed Drives, London, pp. 284-287, May 1984,
4. Murphy, J.M.D., Thyristor Control of A.C. Motors, Pergman Press, pp. 37-68, 1978.
5. Fitzgerald, A.E., Kingsley, C. and Kusko, 'A., Electric Machinery, McGraw-Hill Book Co., pp. 419-424, 1971.

### Appendix:

TOL = Turn-off Limit

ANGLE = Conduction angle

ICOND = 1..Conducting Thyristor

ICOND = 0..non-Conducting Thyristor

IDIOD = 1.. Conducting diode

IDIOD = 0.. non-Conducting diode

ICONDT.. Total number of conducting diodes and Thyristors.

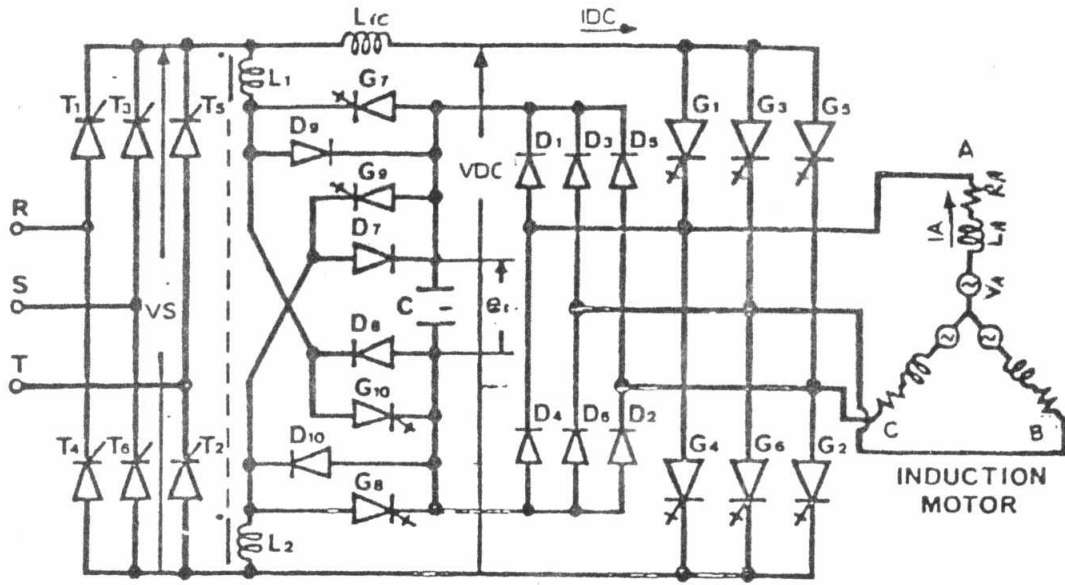
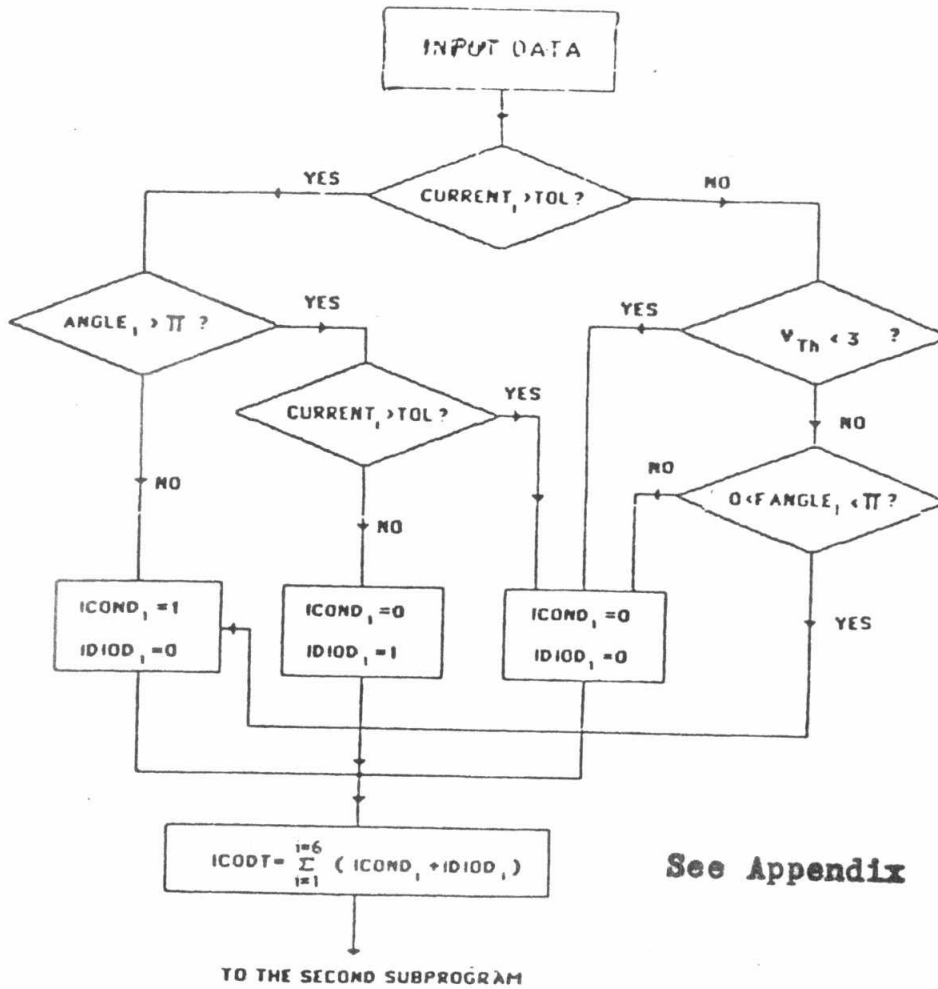


Fig.1. The CSI-GTO inverter configuration.



See Appendix

Fig.2. Logic diagram of individual GTO thyristor.

Table 1. The output variables and the conducting state of each GTO thyristor (ICOND) and Diode (IDIOD)

T	TH1	YD4	TH4	YD1	YL1	TH3	YD6	TH6	YD3	YL2	TH5	YD2	TH2	YD5	YL3	Conducting =1 Blocking =0	
																ICOND	IDIOD
00010	0.0	1.35	0.0	0.0	-1.35	1.07	0.0	0.0	0.0	-1.07	0.0	0.0	2.41	0.0	2.41	011000	000100
00030	0.0	1.20	0.0	0.0	-1.20	1.22	0.0	0.0	0.0	-1.22	0.0	0.0	2.42	0.0	2.42	011000	000100
00050	0.0	1.05	0.0	0.0	-1.05	1.37	0.0	0.0	0.0	-1.37	0.0	0.0	2.42	0.0	2.42	011000	000100
00070	0.0	0.91	0.0	0.0	-0.91	1.51	0.0	0.0	0.0	-1.51	0.0	0.0	2.43	0.0	2.43	011000	000100
00090	0.0	0.77	0.0	0.0	-0.77	1.66	0.0	0.0	0.0	-1.66	0.0	0.0	2.43	0.0	2.43	011000	000100
00110	0.0	0.64	0.0	0.0	-0.64	1.81	0.0	0.0	0.0	-1.81	0.0	0.0	2.44	0.0	2.44	011000	000100
00130	0.0	0.49	0.0	0.0	-0.49	1.88	0.0	0.0	0.0	-1.88	0.0	0.0	0.0	2.37	2.37	001000	000110
00150	0.0	0.33	0.0	0.0	-0.33	1.87	0.0	0.0	0.0	-1.87	0.0	0.0	0.0	2.21	2.21	001000	000110
00170	0.0	0.17	0.0	0.0	-0.17	1.87	0.0	0.0	0.0	-1.87	0.0	0.0	0.0	2.05	2.05	001000	000110
00190	0.0	0.02	0.0	0.0	-0.02	1.88	0.0	0.0	0.0	-1.88	0.0	0.0	0.0	1.89	1.89	001000	000110
00210	0.0	0.0	0.14	0.0	0.14	1.88	0.0	0.0	0.0	-1.88	0.0	0.0	0.0	1.74	1.74	001100	000010
00230	0.0	0.0	0.30	0.0	0.30	1.89	0.0	0.0	0.0	-1.89	0.0	0.0	0.0	1.59	1.59	001100	000010
00250	0.0	0.0	0.45	0.0	0.45	1.90	0.0	0.0	0.0	-1.90	0.0	0.0	0.0	1.45	1.45	001100	000010
00270	0.0	0.0	0.60	0.0	0.60	1.91	0.0	0.0	0.0	-1.91	0.0	0.0	0.0	1.30	1.30	001100	000010
00290	0.0	0.0	0.76	0.0	0.76	1.92	0.0	0.0	0.0	-1.92	0.0	0.0	0.0	1.16	1.16	001100	000010
00310	0.0	0.0	0.91	0.0	0.91	1.94	0.0	0.0	0.0	-1.94	0.0	0.0	0.0	1.03	1.03	001100	000010
00330	0.0	0.0	1.06	0.0	1.06	1.95	0.0	0.0	0.0	-1.95	0.0	0.0	0.0	0.89	0.89	001100	000010
00350	0.0	0.0	1.21	0.0	1.21	1.97	0.0	0.0	0.0	-1.97	0.0	0.0	0.0	0.76	0.76	001100	000010
00370	0.0	0.0	1.36	0.0	1.36	1.99	0.0	0.0	0.0	-1.99	0.0	0.0	0.0	0.63	0.63	001100	000010
00390	0.0	0.0	1.51	0.0	1.51	2.02	0.0	0.0	0.0	-2.02	0.0	0.0	0.0	0.51	0.51	000100	000011
00410	0.0	0.0	1.52	0.0	1.52	2.00	0.0	0.0	0.0	-1.87	0.0	0.0	0.0	0.35	0.35	000100	000011
00430	0.0	0.0	1.53	0.0	1.53	2.00	0.0	0.0	0.0	-1.72	0.0	0.0	0.0	0.19	0.19	000100	000011
00450	0.0	0.0	1.55	0.0	1.55	2.00	0.0	0.0	0.0	-1.58	0.0	0.0	0.0	0.03	0.03	000100	000011
00470	0.0	0.0	1.56	0.0	1.56	2.00	0.0	0.0	0.0	-1.44	0.12	0.0	0.0	0.0	-0.12	000110	000001
00490	0.0	0.0	1.58	0.0	1.58	2.00	0.0	0.0	0.0	-1.30	0.28	0.0	0.0	0.0	-0.28	000110	000001
00510	0.0	0.0	1.60	0.0	1.60	2.00	0.0	0.0	0.0	-1.17	0.43	0.0	0.0	0.0	-0.43	000110	000001

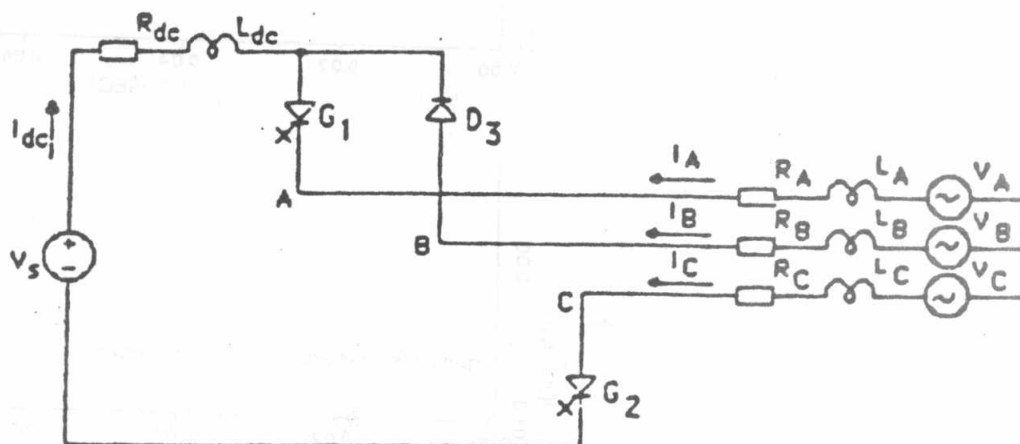


Fig.3.  $G_1, G_2$  and  $D_3$  are conducting.

EE-3 1304

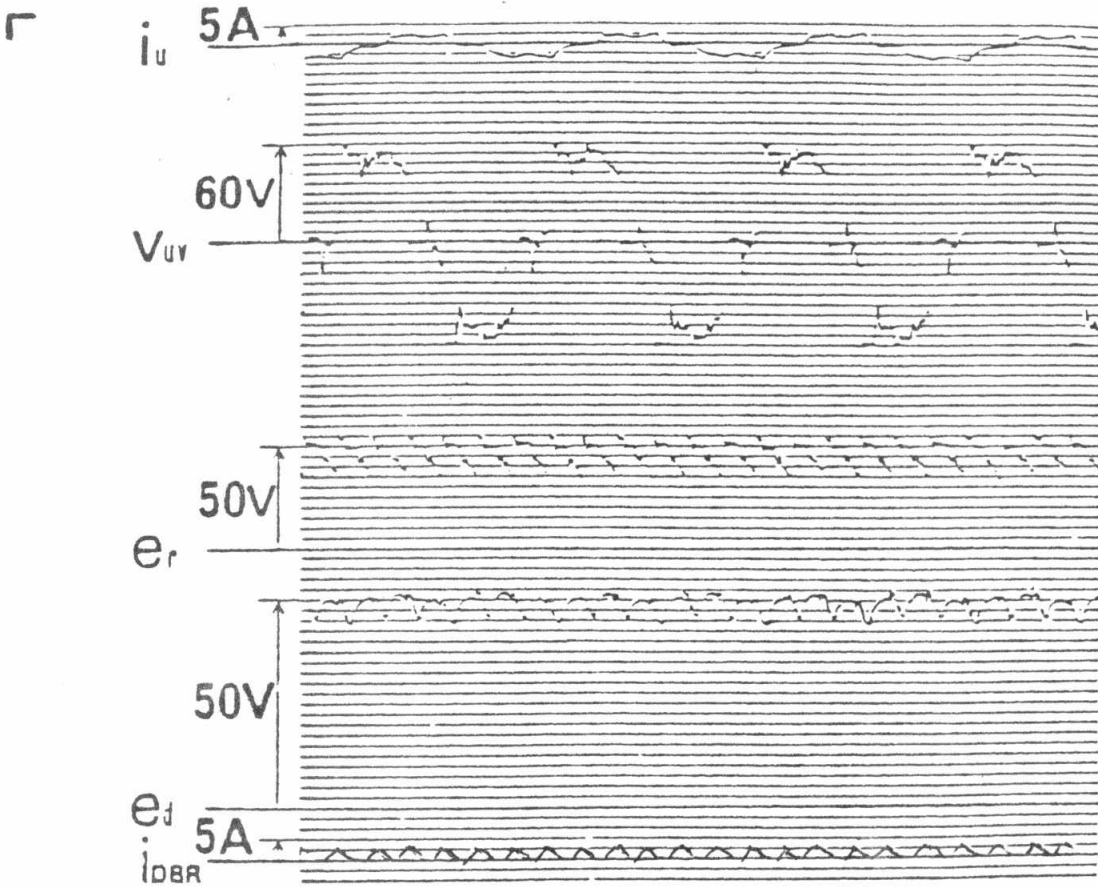


Fig.4. Experimental waveforms of CSI-GTO inverter motor drive system (for comparison), from 3 , p. 287.

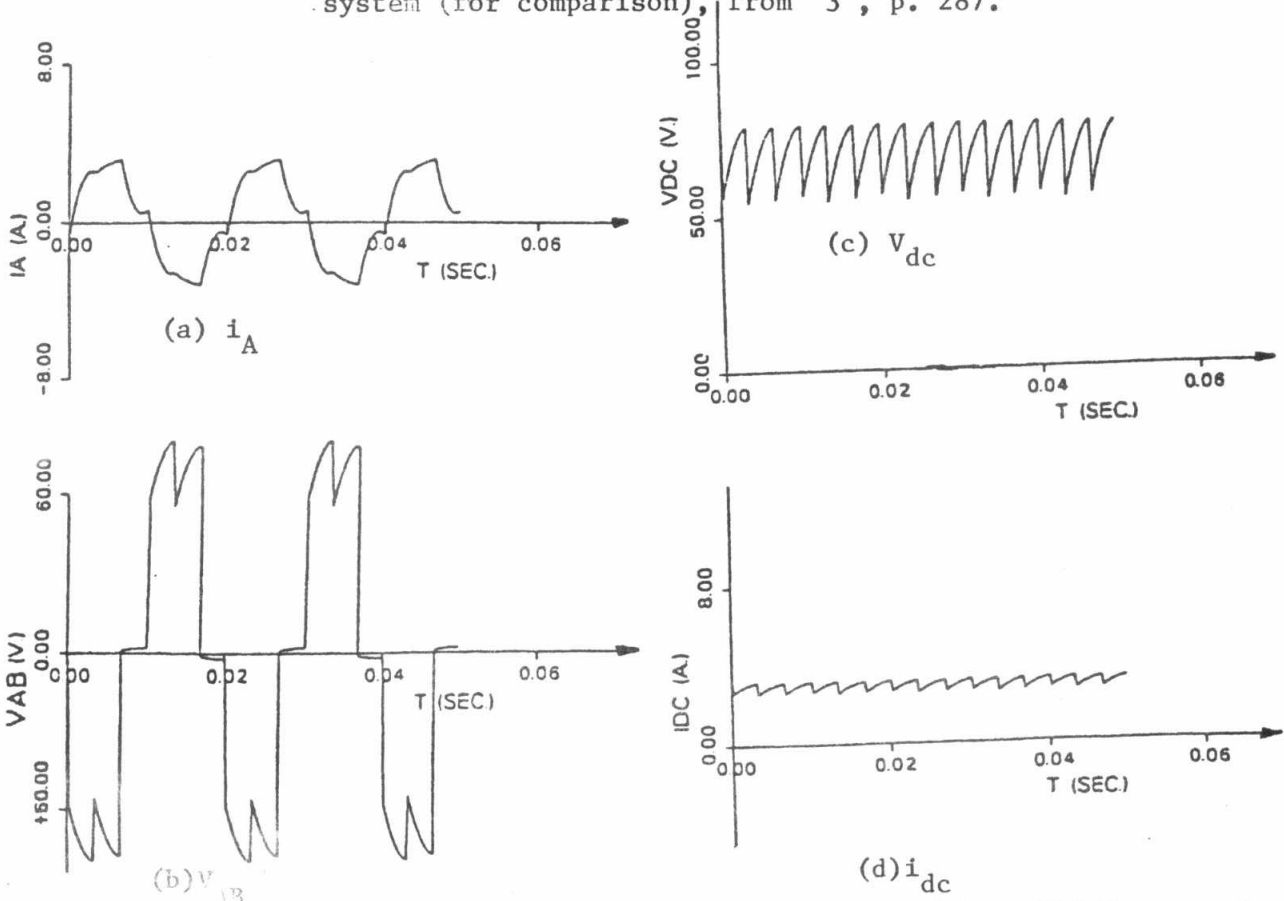


Fig.5. Simulation results of CSI-GTO inverter motor drive system overlaid on the experimental results.



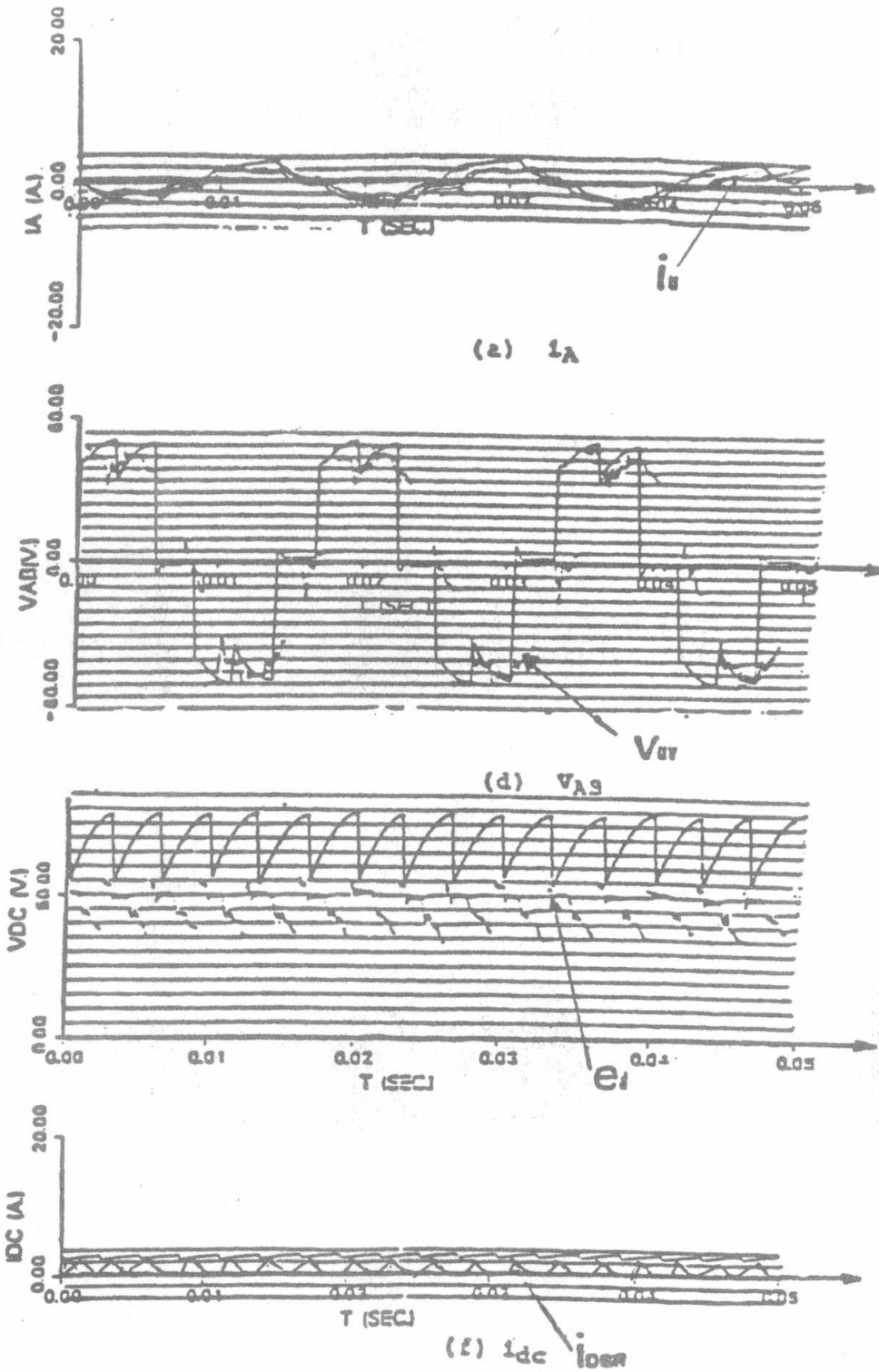


Fig.6. Simulation results of CSI-GTO inverter Motor Drive system overlaid on the experimental results.